Structural motifs of cholesterol nanoparticles

Cromie, S., & Ballone, P. (2009). Structural motifs of cholesterol nanoparticles. Journal of Chemical Physics, 131(3), 034906-1-034906-11. [034906]. DOI: 10.1063/1.3179683

Published in:
Journal of Chemical Physics

Structural motifs of cholesterol nanoparticles

S. R. T. Cromie and P. Ballone[a)]
Atomistic Simulation Centre, Queen's University Belfast, Belfast BT7 1NN, United Kingdom

(Received 28 April 2009; accepted 24 June 2009; published online 21 July 2009)

The growth sequence of gas-phase cholesterol clusters (Ch_N) with up to $N=36$ molecules has been investigated by atomistic simulation based on an empirical force field model. The results of long annealings from high temperature show that the geometric motifs characterizing the structure of pure cholesterol crystals already appear in nanometric aggregates. In all clusters molecules tend to align along a common direction. For cluster sizes above the smallest ones, dispersion interactions among the hydrocarbon body and tails of cholesterol cooperate with hydrogen bonding to give rise to a bilayer structure. Analysis of snapshots from the annealing shows that the condensation of hydrogen bonds into a connected network of rings and chains is an important step in the self-organization of cholesterol clusters. The effect of solvation on the equilibrium properties of medium-size aggregates is investigated by short molecular dynamics simulations for the $N=30$ and $N=40$ clusters in water at near ambient conditions and in supercritical carbon dioxide at $T=400$ K. © *2009 American Institute of Physics*. [DOI: 10.1063/1.3179683]

I. INTRODUCTION

Cholesterol, a well known member of the sterol family, is an essential component of biological membranes and plays an important role in a variety of biological and biochemical processes.[1] In the popular perception, its beneficial effects often are obscured by the health hazard represented by abnormally high cholesterol concentrations, which greatly increase the risk of cardiovascular diseases and potentially lead to infarction and stroke.[2]

Almost without exception, the negative side effects of cholesterol are associated to its precipitation out of oversaturated physiological solutions, giving rise to plaques that clog arteries or producing stones in the gallbladder. The clinical impact of these processes points to the nucleation of cholesterol aggregates as an important topic for biomedical research. The biomedical relevance of nanometric cholesterol aggregates is further increased by the possibility of using lipid,[3] and thus also cholesterol,[4] for innovative drug delivery strategies. Lipid vesicles and micelles, in particular, provide a protective coating for hydrophobic species, while the incorporation into inverted micelles could greatly enhance the translocation rate of hydrophilic species across biomembranes.[5]

At a more fundamental level, pure cholesterol is known to display a fascinating variety of low-dimensional structures (micelles and vesicles) in water solution[6,7] and to crystallize into two distinct forms,[8] whose relative stability depends on temperature, with a solid-solid transition taking place at $T=312$ K.[9,10] Both crystal forms consist of the stacking of compact cholesterol bilayers, stabilized by dispersion forces among the hydrocarbon bodies, and fastened by chainlike arrangements of hydrogen bonds formed by the OH molecular terminations (see Fig. 1). The same forces, i.e., dispersion interactions and hydrogen bonding, drive the aggregation of all other forms of pure cholesterol. Steric considerations and entropy contributions related to the alkane tail, however, play an important role in fine tuning the structure and the properties of the phases observed in cholesterol systems. A similar

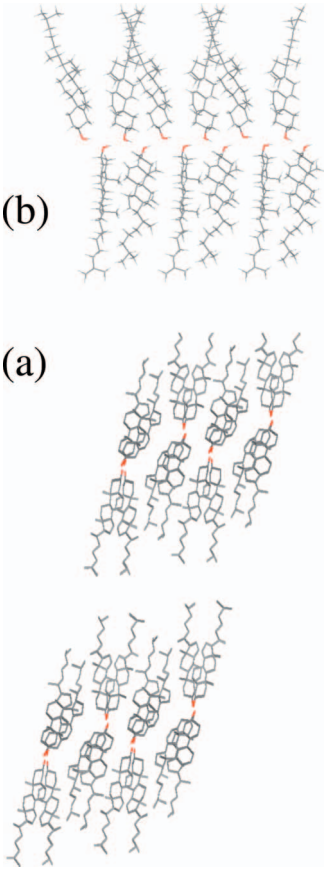

FIG. 1. (a) Perspective view of the low temperature crystal phase of cholesterol. The vertical separation of bilayers has been expanded to visualize the hydrogen-bonding pattern. (b) Side view of the low temperature crystal phase of cholesterol showing the hydrogen-bond pattern. Black atoms and bonds: carbon; red atoms: oxygen; white atoms: hydrogen.

[a)]Electronic mail: p.ballone@qub.ac.uk.

balance of dispersion, steric, and entropic interactions with hydrogen bonding appears to determine also the structure of the several cholesterol-monohydrate crystal forms, which are known from experiments.[11,12]

The variety of forms and shapes resulting from cholesterol aggregation is greatly enhanced if in addition to equilibrium phases we consider nonequilibrium structures produced by sudden precipitation out of supersaturated solutions.[13] The optical properties of cholesterol crystallites arising from these processes display a distinctive biaxial character, resulting from the anisotropic growth within the plane of the bilayers and in the direction of the bilayer stacking. The detailed shape of the crystallites, however, is influenced by a large number of physical and chemical parameters, including temperature, *p*H, electrolyte strength, and quality of the solvent (see Ref. 14). Moreover, nucleation conditions also play a role, and the result of precipitation depends on the quality and concentration of third species in solutions, such as proteins,[15] and can be drastically modified by the presence of interfaces with a solid (mineral) support[16] or with biomembranes.[17] All these considerations emphasize the interest of small cholesterol aggregates, whose thermodynamic and structural properties are important to understand all the phenomena briefly mentioned above.

As a first step, we investigate by computer simulation ground state and thermal properties of gas-phase cholesterol clusters (Ch_N) with up to $N=36$ molecules using an atomistic force field model. The results show that the same combination of dispersion (van der Waals) interactions, hydrogen bonding, steric, and entropy effects that determine the structure of the crystal phases is already at play in nanometric cholesterol aggregates. Moreover, and more importantly, the relative weight of all these factors is similar for clusters and for crystals. As a result, characteristic motifs seen in cholesterol crystals, such as bilayers, linear chains of hydrogen bonds, and a nearly parallel orientation of cholesterol molecules, appear very early in the growth sequence.

The relatively weak cohesion of cholesterol clusters and cholesterol crystals makes them sensitive to interactions with the surrounding medium. Structural properties of nanoaggregates and their detailed growth sequences, in particular, are likely to be greatly affected by solvation. Moreover, because of the amphiphilic properties of cholesterol, the effect of solvation is expected to be qualitatively different for solvents able to accept and/or donate hydrogen bonds, and for hydrophobic solvents, preferentially interacting with the hydrocarbon body of cholesterol.

To provide a first qualitative assessment of the role of solvation, molecular dynamics (MD) simulations have been carried out for an aggregate made of 10, 30, and 40 cholesterol molecules immersed in liquid water and in supercritical carbon dioxide.[18] The size of this cluster is below the range estimated for fully formed micelles (or inverted micelles), exposing a smooth and complete hydrophilic (hydrophobic) surface to the water (CO_2) contact. Nevertheless, the simulation results display the structural and dynamical properties expected for aggregates of amphiphilic molecules solvated in these two fluids of complementary character. In both cases clusters are more globular and far more floppy than in the gas phase.

In the case of water, and especially at relatively low temperature, cholesterol clusters still partly retain structural features characteristic of the gas-phase structures. The microscopic organization of gas-phase and water solvated clusters, however, is drastically different since in the former case the OH termination of cholesterol points toward the center of the cluster, while in the latter it points outward partly because of slightly stronger hydrogen bonding with water and certainly stabilized also by entropic effects.

Our simulations for cholesterol clusters in supercritical CO_2 have been carried out at fairly high temperature and pressure ($T \geq 400$ K, $P \geq 1.2$ kbar), far from the conditions used in extraction processes (see Ref. 19) and approaching those used to dissolve a sizable amount of cholesterol[20] as a preliminary stage in the generation of nanometric aggregates in a beam by supersonic expansion.[21] At these conditions, similarities with the gas-phase configuration can hardly be recognized partly because of high temperature and because of strong and rapidly fluctuating interactions with the solvent. In this last case, cholesterol molecules are still predominantly oriented along the radial direction, diverging from the center of mass of the cluster. However, the OH terminations of cholesterol are nearly uniformly distributed over the entire cluster volume, and hydrogen bonding is nearly irrelevant. The results of these simulations for medium-size solvated aggregates complement the information provided by a recent computational investigation of cholesterol clusters adsorbed at the surface of water.[22]

Unfortunately, no experimental data are available for comparison with the computational results, especially for gas-phase clusters. However, nanometric cholesterol aggregates free of interactions with a solid substrate or with a solvent could be produced by advanced beam techniques[23] and then stored in an ion-trap (upon complexation with a charged partner) and investigated by optical spectroscopy.[24]

A sizable and growing amount of chemical physics data is instead available for clusters solvated in water.[7] Moreover, the nucleation of cholesterol solids out of a water solution has been investigated by grazing x-ray diffraction in Ref. 25.

II. THE MODEL AND THE SIMULATION METHOD

Cholesterol is a relatively simple organic molecule, consisting of a nearly saturated hydrocarbon frame with a OH group (alcohol termination; see Fig. 2). The hydrocarbon frame, in turn, can be divided into a polycyclic body and a fairly flexible alkane tail. The nearly planar symmetry of the polycyclic body is broken by two methyl groups sticking out of the same (β–) side of the molecule, while the opposite (α–) side is relatively flat.

The intramolecular backbone of covalent bonds appears to be nearly free of strain, apart from a slight distortion of the fivefold ring $C_{13}-\ldots-C_{17}$ and an even smaller deformation of the $C_5-\ldots-C_{10}$ sixfold ring due to the double bond between C_5 and C_6. Moreover, the electronic polarizability of cholesterol is relatively low (especially considering the mo-

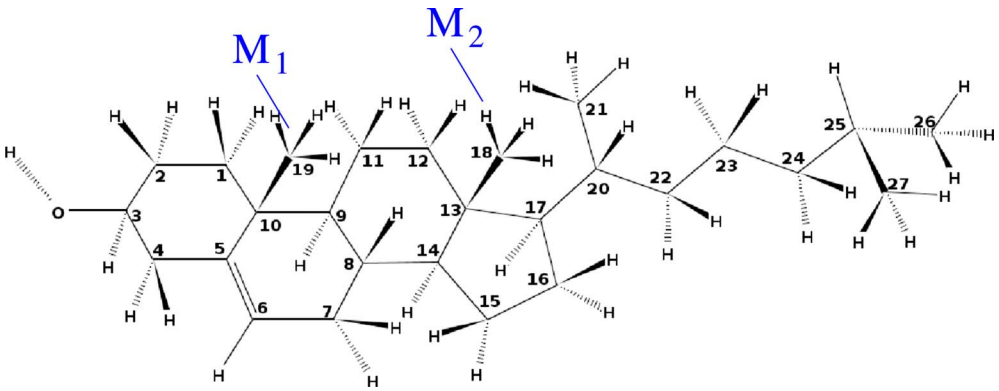

FIG. 2. Schematic drawing of the cholesterol molecule.

lecular size), as shown by the small value of the high frequency dielectric constant ($\epsilon_\infty \sim 2$) for liquid and solid phases of cholesterol and closely related derivatives.[26] From the point of view of molecular modeling, therefore, cholesterol appears an almost ideal candidate for empirical force field approaches, and several generic models could be used to simulate cholesterol molecules. Moreover, specific models have already been developed and tested,[27] giving satisfactory results. Nevertheless, we use an all-atom interatomic potential developed by us, and described in Ref. 22, partly for consistency with our investigation of cholesterol islands on water and partly for its compatibility with the DL_POLY (Ref. 28) molecular dynamics package used for a portion of our computations.

Geometric constraints and, to a lesser extent, the isolated $C_5=C_6$ double bond impart a remarkable rigidity to the macrocyclic body of cholesterol. As a result, the atom by atom description of cholesterol is highly redundant; the dynamical and the thermodynamic properties of this molecule are far more efficiently described by a few collective variables giving the center of mass position, the orientation of the main body, and the rotational isomer of the tail. Monte Carlo (MC) approaches have distinct advantages in incorporating these features into an efficient sampling scheme, and this consideration has played a major role in our choice of the simulation method.

The primary computational tool used to optimize the structure of pure cholesterol cluster has been represented by Monte Carlo simulation. We used a program developed in house, including a sequence of multiatom moves required to sample efficiently the rugged energy landscape of these molecules. The moves include rigid translation and rotation of whole molecules, the rotation of all different segments of the alkane tail, the rotation of the OH group, as well as single-atom displacements to locally relax the atomistic structure. All moves and acceptance rules are consistent with the basic principles of Monte Carlo simulations. In particular, to ensure microscopic reversibility, the succession of different moves is selected at random. On average, a full set of multiatom moves is performed for every single-atom attempted displacement. In what follows, the length of the MC runs is measured by the number of attempted single-atom displacement. It is important to realize, however, that this corresponds to a larger number of attempted changes for the relevant collective coordinates, resulting in significant acceptance ratios and large mean square displacements even at fairly low T. In many respects, our MC implementation emphasizing multiatom over single-atom moves represents an intermediate stage in between atomistic and coarse grained models.

The MC optimization is carried out by simulated annealing, i.e., by first equilibrating the systems at $T=600$ K and then reducing T in steps of 20 K. The amplitude of the attempted displacements and rotations are progressively reduced with decreasing T to maintain the corresponding acceptance ratios in the 0.3–0.5 range. The starting temperature is only slightly below the boiling point of cholesterol and also close to the temperature at which it thermally decomposes. This last change, of course, does not affect simulation since our potential does not allow covalent bonds breaking. Clusters nucleate quickly already for $500 \leq T \leq 600$ K and coalescence into a unique aggregate, which takes place for $450 \leq T \leq 500$ K. Evaporation of molecules during the first stages ($T \leq 450$) of the annealing is prevented by the application of a weak quadratic potential at distances $R \geq 50$ Å from the origin. Simulations are discarded (or the temperature is raised again to $T=600$ K) if the sample is still divided into different aggregates below $T=450$ K. The experimental melting temperature of bulk cholesterol is $T_M=423$ K,[12] and molecules are expected to maintain high molecular mobility down to fairly low temperatures in clusters of nanometric size. Each annealing cycle consists of $\sim 200 \times 10^6$ single particle MC moves. Thermal averages reported in the following sections have been computed over at least 2×10^6 MC moves.

At the lowest temperature range ($T < 80$ K), however, even collective modes are frozen out, and single-atom displacements are very ineffective in minimizing the energy. Therefore, the MC annealing cycle is complemented by a quenched molecular dynamics energy minimization carried out with the DL_POLY package.[28]

The annealing is repeated about ten times for every cluster size, starting from a different random configuration or reheating the result of previous annealings. Computational time scaled nearly linearly with cluster size upon limiting the range of all interactions to 12 Å, and the annealing of a medium-size cluster ($N=24$) requires about 10 days on a

single OPTERON CPU. Simulations for different cluster sizes and different starting points for the same size have been distributed over many CPUs, but no effort has been made to parallelize the MC code.

Needless to say, we do not think that our relatively simple simulated annealing strategy provides a certain or even a very likely identification of the absolute energy minimum for any size above the smallest ones. In fact, even for much simpler systems, much more sophisticated methods[29] are required for a thorough characterization of the potential energy surface of clusters. Nevertheless, our method, based on the characteristic geometric and dynamical properties of the cholesterol molecule, provides a coherent picture of bonding for these systems, and the systematic trends and common geometric motifs found by simulation support our claim of having identified the important features in the growth sequence of cholesterol clusters. Our confidence of having at least identified representative low-energy structures is enhanced by the observation that for any given size, all annealings produce geometries whose energy per cholesterol molecule is well within 4 kJ/mol from the most stable one. For instance, the standard deviation of the resulting energy per particle for the $N=20$ cluster turns out to be 2 kJ/mol. Moreover, the analysis of the acceptance ratio for the different move types and of the related mean square displacements confirms that our MC procedure is very effective in sampling the collective coordinates that describe the clusters' configuration. Test runs carried out using molecular dynamics show that the frequency of events, such as molecular reorientation, rotational isomerization, and large elongation molecular displacements, takes place at a frequency that is far too low for a method whose time step is limited by the high frequency atomic dynamics. On the other hand, the relative merit of MD and MC strongly depends on cluster size since the likelihood of accepting long elongation multiatom displacements is large for the moderately coordinated molecules in small clusters and negligible for the highly coordinated molecules at the center of medium and large clusters. Therefore, the $1 < N \leq 36$ size range we investigated probably is the largest that can be efficiently explored by MC.

The advantage of MC over MD turns into a disadvantage also in the case that a medium-size molecule such as cholesterol is solvated into a liquid made of small molecules such as water or CO_2 because the presence of the small molecular species will limit the elongation of acceptable displacements or isomerization rate for the larger species. For this reason, clusters solvated in water and in supercritical CO_2 have been simulated by molecular dynamics using again the DL_POLY package.[28] In the case of CO_2 we used a simulation cell with 3000 CO_2 molecules. In the case of water, the cholesterol cluster was surrounded by 2850 water molecules. Most simulations have been carried out in the *NPT* ensemble with a time step of 1 fs. The only exception is represented by the simulation of Ch_{10} in water carried out at *NVT* conditions.

Water is described by the flexible-bonds three-center potential in Ref. 30, whose properties are well documented in the literature. The water-cholesterol cross interactions deviate somewhat from the ideal Berthelot rules (see the detailed discussion in Ref. 22) to compensate for an apparent overestimation of the cholesterol-water intermixing observed in our computation for cholesterol islands when using the standard (Berthelot) combination of nonbonded interactions.

Carbon dioxide is also described by a flexible-bonds three-center potential, starting from the parametrization proposed in Ref. 31. Also in the case of CO_2, the nonbonded cross interaction with cholesterol deviates somewhat from Berthelot's rule. Modifications have been introduced to restore the qualitative agreement of simulation with known experimental facts. More precisely, experimental measurements have shown that cholesterol gives rise to (dynamically) stable aggregates in supercritical CO_2.[18] Preliminary simulations for cholesterol clusters in supercritical CO_2 carried out with the CO_2 potential in Ref. 31 and the cholesterol potential in Ref. 22 combined via Berthelot's rule, however, have shown that cholesterol clusters quickly dissolve at supercritical CO_2 conditions even at concentrations far above the experimental equilibrium solubility at the temperature and pressure of the simulation. To stabilize cholesterol clusters, therefore, we changed the Lennard–Jones cross interactions into

$$V_{LJ}(r) = 4\epsilon' \left[\left(\frac{\sigma}{r} \right)^{12} - \delta \left(\frac{\sigma}{r} \right)^{6} \right], \tag{1}$$

where $\delta=0.95$ and ϵ' is 80% of the value corresponding to Berthelot's rule. Clusters in solution have been equilibrated for at least 4 ns, and statistics has been accumulated during a further run of 7 ns in the case of water and 4 ns in the case of CO_2.

III. SIMULATION RESULTS

A. Gas-phase clusters

Gas-phase cholesterol clusters with up to $N=36$ have been simulated. Each annealing started from a random geometry, with molecules uniformly distributed within a sphere of radius $R=40$ Å and with nearly isotropic orientation of the main molecular axis. No periodic boundary conditions are applied in simulations for the gas-phase clusters. Starting from this vapor configuration, clusters form in the early stages of the annealing and progressively acquire a fairly regular geometry with temperature decreasing to nearly 0 K. The average potential energy decreases monotonically and nearly linearly with decreasing T. The precise identification of the different stages of cluster formation and ordering by thermodynamics means is unfortunately prevented by large fluctuations at high T and by the limited value of the potential energy or specific heat variations associated to these processes. As already mentioned in Sec. II, the MC annealing is continued down to $T=20$ K, but below $T \sim 80$ K the method is rather ineffective in removing the residual energy, and a final stage of structural optimization by quenched MD is needed to obtain reliable energies for the structures identified by MC.

We first discuss the structural information since this gives us a basis for the interpretation of the cohesive energy data. A general observation, valid for all low-energy structures, is that molecules tend to align their longer axis along a common direction apparently because of the elongated shape

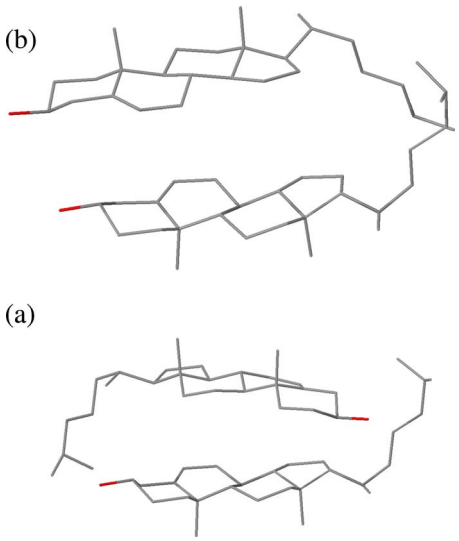

FIG. 3. Low-energy structures of the cholesterol dimer. The lowest energy configuration corresponds to (a). Only nonhydrogen atoms are shown.

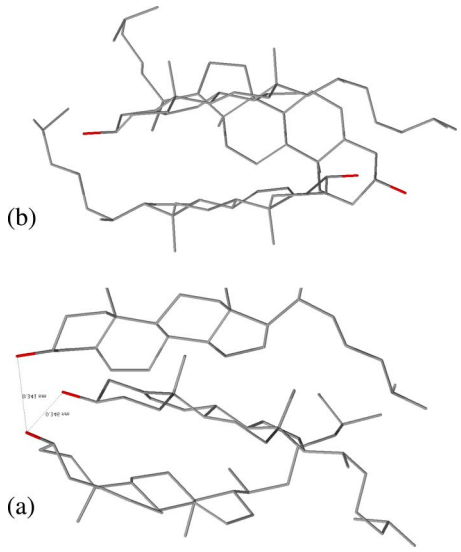

FIG. 4. Low-energy structures of the cholesterol trimer. Only nonhydrogen atoms are shown.

of cholesterol. This feature anticipates the important role of crystal liquid states in the phase diagram of cholesterol and of closely related cholesterol derivatives.[32]

The lowest energy structure of the cholesterol dimer is illustrated in Fig. 3. The two molecules are joined through their flat α-side with their tails folded toward the OH termination of the partner molecule. Pairs of cholesterol molecules joined by their α-sides are an important structural motif in cholesterol crystals and appears also in our simulation results for dense cholesterol films on water.[33] The hydrogen-bonded version of Ch_2, illustrated in Fig. 3(b), is 13 kJ/mol higher in energy than the ground state. The hydrogen bond is relatively weak, with an O–O distance of 3.91 Å, apparently strained by competing dispersion and steric interactions. The Ch_2 ground state geometry only rarely appears in the low-energy structure of larger clusters as a clearly identifiable motif. The dimer geometry shown in Fig. 3(b) instead can be identified in clusters up to fairly large sizes. This difference might be related to a different ability of these two configurations to give rise to more extended structures under the effect of dispersion forces.

Hydrogen bonding first appears as a relevant ground state feature in the cholesterol trimer, whose lowest energy structure [shown in Fig. 4(a)] is characterized by two connected hydrogen bonds. In both cases the O–H–O configuration is nearly linear, but the O–O distance (d_{OO}=3.45 Å) is fairly long, pointing to strained and relatively weak hydrogen bonds. The two hydrogen bonds of Ch_3 form an angle of 92°, somewhat narrower than the 109° expected for tetrahedral bonding around each of the oxygen atoms. Not surprisingly, the short chain of hydrogen bonds does not close onto itself since the 60° angles required for such a triangular configuration would represent a major distortion of the already strained bonding around the O atoms. As a result, the three O atoms (and the corresponding Ch molecules) are all inequivalent, since one acts exclusively as a hydrogen-bond donor, one as a hydrogen-bond acceptor, while the third one both accepts and donates a hydrogen bond. A different configuration of Ch_3, illustrated in Fig. 4(b) and having only one hydrogen bond, is more appropriately described as a 2+1 cluster. Its energy is less than 8 kJ/mol higher than that of the lowest energy structure, emphasizing the remarkable stability of the Ch_2 dimer, nearly compensating the loss of a (weak) hydrogen bond.

The interplay of hydrogen bonding, dispersion interactions, and steric considerations is apparent also in the lowest energy structure found for Ch_4 (see Fig. 5). As expected, the axes of the four molecules are nearly parallel to each other. The four OH groups are exposed on one side of the Ch_4 elongated structure and form two distinct and rather weak hydrogen bonds with an O–O distance of 3.80 Å. The two hydrogen bonds are too separated from each other (O–O distance of about 6 Å) to interact. A closer look, in fact, shows that the cluster can be described as consisting of two Ch_2 pairs, each adopting a geometry similar to the one in Fig. 3(b), bound by dispersion forces.

No new motifs appear in the low-energy structures found for Ch_5 and Ch_6 by our simulations. For these two sizes, in fact, all the low-energy geometries can be seen as obtained by combining Ch_2 and Ch_3 units in the geometries described above.

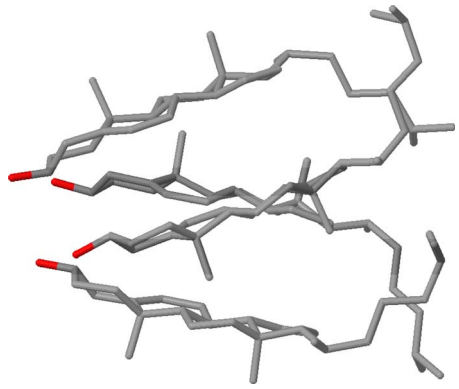

FIG. 5. Lowest energy structure of the cholesterol tetramer. Only nonhydrogen atoms are shown.

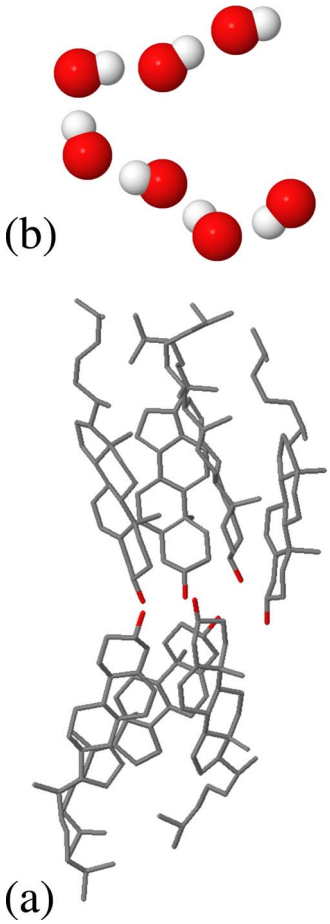

FIG. 6. Lowest energy structure for Ch_7. (a) Side view. (b) Hydrogen bonds' configuration.

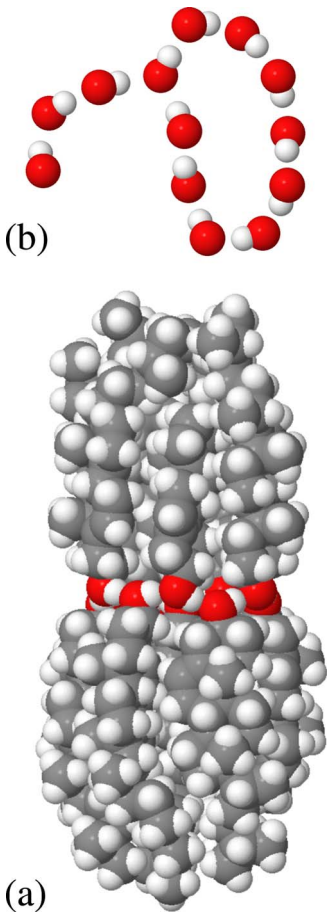

FIG. 7. Lowest energy structure of the Ch_{13} cluster. (a) Side view. (b) Hydrogen bonds' configuration.

Two related new features instead appear simultaneously with Ch_7, whose lowest energy configuration shows a geometry reminiscent of the double layer structure of extended phases. As can be seen in Fig. 6, the molecular axes are orthogonal to a common plane that divides the cluster into two unequal parts. All OH terminations of the cholesterol molecules are adjacent to the equatorial plane, giving rise to a folded chain of hydrogen bonds. The arrangement of the OH groups in the equatorial plane is shown in Fig. 6(b). All O–O distances are less than 2.90 Å, pointing to strong hydrogen bonds. The alternate location of cholesterol molecules with respect to the central plane plays an important role in promoting the formation of the hydrogen-bond chain, unhindered by steric constraints that would instead arise from a one sided geometry. In fact, only molecules on opposite sides of the central plane are able to form strong hydrogen bonds.

The hints of double layer structure that appear with Ch_7 are fully developed for $N \geq 10$. In this respect, the Ch_{13} structure shown in Fig. 7 can be considered as representative of medium-size clusters up to $N=20$. In all cases, clusters display a clear equatorial plane hosting the OH groups. Molecules are arranged on the two sides of the OH location, with their axes perpendicular to the equatorial plane. The high density of OH groups in this plane favors the formation of long hydrogen-bond chains that sometimes close themselves into rings. Moreover, especially for $N>10$, the hydrogen-bond chains often display branching. Both features are apparent in the hydrogen-bond configuration of Ch_{13} displayed in Fig. 7(b). Analysis of the different energy contributions shows that for $N>6$, hydrogen-bonding accounts for $\sim 25\%$ of the cluster cohesive energy. On the other hand, the short range and directionality of hydrogen bonding make this contribution very sensitive to the atomistic structure of the aggregate. Analysis of simulation snapshots selected at different temperatures during the annealing shows that the condensation of hydrogen bonds into a connected structure takes place around $T=320$ K.

Needless to say, not all lowest energy structures found by our simulations strictly conform to these simple rules. Deviations from the picture describe above, in fact, become more frequent with increasing cluster size possibly because of limitations in our optimization strategy that become more severe with increasing N or, perhaps, because of the competing effect of different bonding and packing patterns. In some cases, for instance, one molecule appears to be antiparallel to the local prevailing orientation, pointing its OH termination away from the equatorial plane. Very likely, this is a defect resulting from incomplete optimization. However, reversing the Ch orientation by hands and briefly reoptimizing the configuration always gave rise to configurations of slightly higher energy. In some other cases, one molecule lies in the equatorial plane, wrapped around the central disk of OH ter-

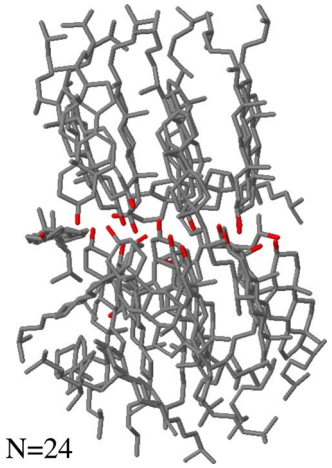

FIG. 8. Lowest energy structure of the Ch_{24} cluster. Only nonhydrogen atoms are shown.

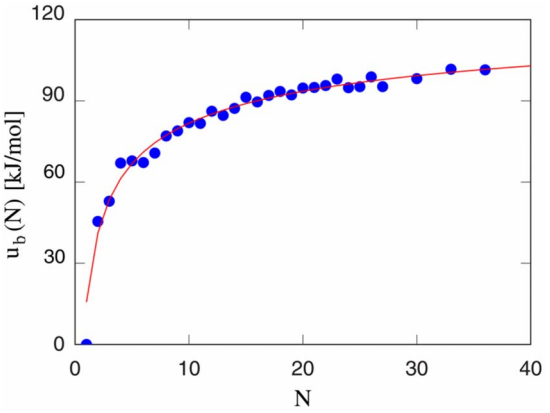

FIG. 9. Binding energy per molecule u_b as a function of cluster size N. Dots: simulation results. Full line: interpolation with the expression given in Eq. (2).

minations. Also in these cases, the observed configuration is likely to be an artifact of incomplete optimization, but the relatively high frequency of this geometry suggests that it might have some reason of stability.

The fairly high frequency of the defective structures described above gives a slightly more globular character to the lowest energy structure of clusters with more than 20 molecules (see, for instance, $N=24$ in Fig. 8), as opposed to the more discoidal geometry of clusters with $10 \leq N \leq 20$. Nevertheless the equatorial disk of OH groups and hydrogen bonds is always apparent, and long, curved, and often branched hydrogen-bond chains are always seen in low-energy geometries. These considerations apply up to the largest size we investigated, i.e., up to $N=36$.

The most direct measure of the cluster morphology might be given by the distribution of the principal momenta of inertia for the aggregates that display a clear separation between two large momenta, and a smaller one, as expected for oblate ellipsoids. Transitions from oblate to prolate ellipsoid and eventually to spheroidal aggregates are expected to take place with increasing cluster size.[34]

The lowest energy U obtained for each cluster size N is combined with the ground state energy of the single cholesterol molecule to compute the cohesive energy per molecule defined as $u_b(N)=-[U(N)-N\times U(1)]/N$. The results are shown in Fig. 9. As apparent from the figure, the size dependence of u_b displays a downward curvature, providing information on the surface energy of small cholesterol clusters. The simulation data are interpolated by the expression

$$u_b(N) = \frac{1}{N}[aN - bN^{2/3}]. \tag{2}$$

This analytic fit corresponds to a spherical aggregate of cohesive energy a and surface tension

$$\gamma = \left(\frac{4\pi}{3V_1}\right)^{2/3} \frac{b}{4\pi}, \tag{3}$$

where V_1 is the volume per cholesterol molecule in the low temperature crystal phase. The form of the interpolation is suggested by the approximately globular shape of the optimized clusters, and it provides an excellent fit to the simulation data (dots in Fig. 9), as shown by comparison with the continuous line representing the analytic interpolation.

The $N \to \infty$ limit of $u_b(N)$, corresponding to the coefficient a of the fit, provides an estimate for the cohesive energy of extended system. The result, i.e., $e_b=142$ kJ/mol, turns out to be in fair agreement with the cohesive energy $e_b=151$ kJ/mol computed with the same potential for the low temperature crystal phase of cholesterol. The agreement turns out to be excellent if the bilayer-bilayer interaction, present in the crystal phase and absent in the clusters, is separately accounted for. On the other hand, it is apparent that clusters with up to $N=36$ molecules are still very far from the macroscopic limit, their cohesive energy per molecule being only ~60% of the crystal limit. This observation is somewhat surprising given the apparent short range of the intermolecular interactions. The estimate of the surface tension provided by Eq. (3) turns out to be $\gamma=0.037$ kJ/m^2.

The discoidal shape of clusters for $7 \leq N \leq 20$ suggests other forms for the analytic fit. All attempts, however, give interpolations whose χ^2 is practically indistinguishable or even worse than the one given by Eq. (2).

The simulation results for $u_b(N)$ can be represented as the combination of a regular part expressed, for instance, by the analytic fit of Eq. (2), with a few peaks and dips superimposed to it. Beyond the very small sizes, the interpretation of this oscillating component of $u_b(N)$ is not immediate, and, in particular, it is not possible to identify a sequence of *magic numbers* arising from a well defined two-dimensional (2D) packing sequence.

Below $T \sim 500$ K the temperature dependence of the average potential energy is nearly linear for all cluster sizes. Only for the largest aggregates, the results display slight deviations from linearity that might point to an incipient liquid-solid transition broadened by finite size effects. For $N \geq 20$ this broad anomaly is located at $T \sim 320$ K, and it might be related, at least in part, to the formation of the hydrogen-bond network. These qualitative observations are confirmed by the results for $N=24$ shown in Fig. 10. The deviation of the average potential energy per particle $u(T)$ from linearity is emphasized by subtracting from $u(T)$ a linear contribution

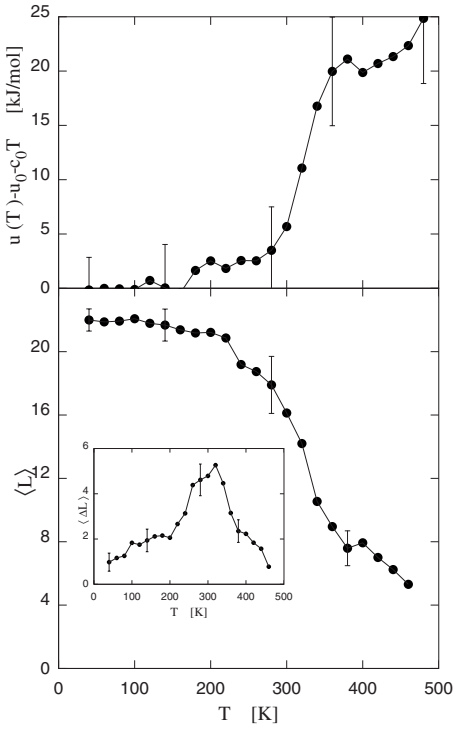

FIG. 10. Upper panel: average potential energy per cholesterol molecules $u(T)$ as a function of T. A linear term u_0+c_0T, approximating the low-T portion of $u(T)$, has been subtracted (see text). Lower panel: average length $\langle L\rangle$ of connected hydrogen-bond chains as a function of temperature. Only chains or rings with more than three members have been considered. Inset: standard deviation $\langle \Delta L\rangle$ of the chain length $\langle L\rangle$ as a function of T. Representative error bars are shown. Lines are a guide to the eyes.

(u_0+c_0T), approximating the low-temperature portion of $u(T)$ (see Fig. 10, top panel). The temperature range of the potential energy anomaly corresponds to the temperatures at which chains of H-bonds organize themselves, as shown by the plot of the average chain length $\langle L\rangle$ as a function of T (see Fig. 10, top panel). The average length $\langle L\rangle$ has been computed by first identifying connected clusters of hydrogen bonds and then averaging over all clusters whose size is larger than three molecules. Further information is provided by the computation of the standard deviation $\langle \Delta L\rangle$ of the average length $\langle L\rangle$, shown in the inset of Fig. 10. The broad peak of $\langle \Delta L\rangle$ at $T\sim 320$ K could be seen, in fact, as a measure of the specific heat contribution due to the formation of hydrogen-bond chains. Analysis of dihedral angles in the alkane tail shows that a large number of rotational isomers are populated even at low temperature, confirming that a sizable amount of entropy arises from the configuration of the tail.

IV. CHOLESTEROL CLUSTERS IN LIQUID WATER AND IN SUPERCRITICAL CO_2

The structural features and general properties discussed in Sec. III A for low-temperature gas-phase clusters are, not surprisingly, greatly modified by solvation in H_2O and in CO_2 above room temperature. The special case of small cholesterol clusters ($N\leq 10$) adsorbed on the liquid water surface at $T=280$ K has been investigated in detail in Ref. 22. The results show that in this case cholesterol forms 2D aggregates with molecules lying flat on the water surface. The surface confinement and the cholesterol aggregation are driven by both potential energy and entropy contributions. The water-cholesterol interaction is fairly strong, and the cluster adsorption is accompanied by a sizable distortion of the planar surface of water.

Simulations for cholesterol in liquid water have been carried out for two cluster sizes, i.e., $N=30$ and $N=40$, at $T=320$ K and $T=350$ K. Limited simulation has been carried out also for $N=10$ at $T=320$ K to provide an upper bound for the saturation concentration of cholesterol in water at the conditions of our simulation. Starting configurations have been obtained by cutting a finite portion of an extended bilayer in water, whose simulation is reported in Ref. 33. Each sample is equilibrated over 4 ns before statistics is accumulated during NPT runs of 7 ns at $P=1$ atm. Running averages of structural and thermodynamic properties do not show any apparent drift after equilibration.

At both temperatures all clusters, including the $N=10$ case, appear to be well defined and stable over simulation times of several nanoseconds, confirming that the saturation concentration is low, as expected for a compound whose molecular solubility is negligible, and dissolves in water only in the form of micelles and vesicles.

The analysis of animations extracted from the simulation trajectory reveals a few similarities with the structural features already seen in the gas-phase clusters. Cholesterol molecules, in particular, still display a fair degree of parallel alignment along a common direction and are arranged on an approximately two-layer geometry. The discoidal character displayed by gas-phase clusters is partly retained by solvated clusters, even though their average structure appears to be somewhat rounded by thermal motion and by the interaction with water. Despite these similarities, however, the organization of cholesterol aggregates in water is very different from that of gas-phase clusters. In the gas phase, for instance, the intralayer plane is occupied by the OH groups, whose hydrogen bonds represent a sizable source of cohesion. In water solvated clusters the molecular orientation is reversed, and the center of the aggregate is occupied by the hydrocarbon body and tail of cholesterol molecules, where they are relatively protected from contact with water. The OH groups, in this case, are oriented outward, stabilized by a fairly high number of hydrogen bonds with water. The formation of a complete hydrophilic surface, characteristic of micelles, is still prevented by the small cluster size, and limited water/hydrocarbon contact takes place at the lateral surface of the discoidal aggregates.

Down to $T=320$, cholesterol molecules display a nonnegligible mobility with respect to each other, and also the isomerization rate of their tail is sizable. As a result, clusters appear to be liquidlike, or, taking into account the prevalent parallel orientation of molecules, they appear to be in liquid-crystal state. The fairly high mobility of cholesterol molecules enhances our confidence in the equilibration of the simulated samples. The fluid state of the organic aggregates is confirmed by the plot of the average density of cholesterol atoms (all included) around the cluster center of mass [see Fig. 11 for $N=30$ and $T=350$ K) that does not display any apparent structure besides the smooth drop-off at the cluster

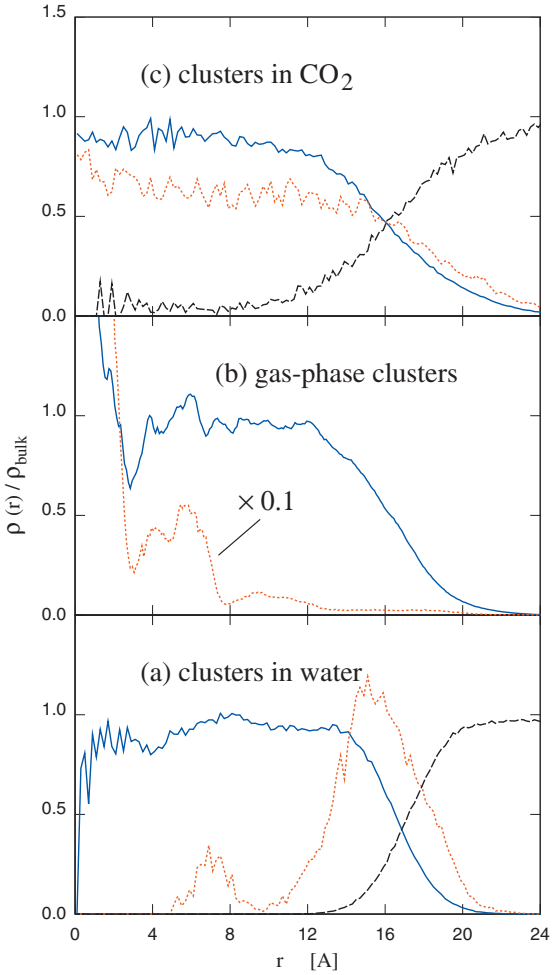

FIG. 11. Density distribution of cholesterol atoms around the center of mass of the Ch_{30} cluster (a) in water at $T=320$ K, (b) gas phase at $T=320$ K, and (c) in CO_2 at $T=400$ K. Full line (blue): carbon atoms of cholesterol; dotted line (red): oxygen of cholesterol; dashed line (black): water oxygen in panel (a), CO_2 carbon in panel (c). Each density has been divided by the density of the same species at the same thermodynamic state, i.e., low-temperature crystal phase for cholesterol carbon, liquid water for water oxygen, and supercritical CO_2 for CO_2 carbon.

boundary. Moreover, the average density in the central portion of the cluster is relatively close to (>92%) the value measured in the equilibrium crystal phase at room temperature.

For both cluster sizes and temperatures, the cholesterol-water interface is fairly broad, as a consequence of (i) the liquidlike character of solvent and solute, (ii) the low interfacial tension, and also (iii) the nonspherical shape of the aggregates. The combined effect of (i)–(iii) can be quantified by computing the 90–10 length (Δ_{10}^{90}) of the interface, defined as the width of the region over which the density drops from 90% to 10% of the bulk value. To within the estimated error bar, this width turns out to be the same ($\Delta_{10}^{90}=5\pm1$ Å) for the $N=30$ and $N=40$ cholesterol clusters in water at the conditions of our simulations. The distribution of water oxygens around the cluster center of mass shows a significant overlap with the cholesterol atoms density partly because of the nonspherical shape of the aggregates and, more importantly, because of the attractive interaction with the cholesterol OH groups. Water, however, is excluded from the central portion of the cluster.

The width of the surface region for gas-phase clusters, shown in the upper panel of Fig. 11 for a comparison, is somewhat broader than in the case of water solvated aggregates apparently because of the discoidal character of the gas-phase structure that is retained even at $T=350$ K. The most interesting feature displayed by the simulation results, however, is the density distribution for the O of cholesterol, displaying a peak at the cluster boundary, as shown in Fig. 11. This contrasts with the result for the gas-phase clusters, also shown in Fig. 11, whose OH density is peaked at the center. This clear inversion of the cholesterol orientation is the most apparent effect of solvation into water, and as already anticipated, it is due to the formation of hydrogen bonds with water. On average, each cholesterol molecule is engaged in 1.2 hydrogen bonds either as donor or as acceptor. The great majority of these bonds connects cholesterol and water, while cholesterol-cholesterol hydrogen bonding is very rare.

Carbon dioxide is a vapor at the conditions considered for cholesterol in water, with a density that is too low to greatly affect the state of the clusters. Partly for this reason and, more importantly, because of the interest arising from applications,[35] simulations have been carried out for the $N=30$ cluster in CO_2 at $T=400$ K and $P=1.2$ Kbar in the supercritical region of the CO_2 phase diagram. Additional computations have been carried out for the same cluster at $T=490$ K and $P=5$ Kbar, a state lying on the same adiabat of the previous one. The equation of state has been computed following Ref. 36. Once again, we emphasize that these conditions correspond to higher temperature and higher pressure than those used in extraction processes or in experiments aiming at solvating functional biological systems. High T and high P have been adopted here partly to enhance the cholesterol-solvent coupling and thus to speed up equilibration and partly to investigate the conditions of cluster formation during adiabatic supersonic expansion from concentrated cholesterol/CO_2 mixtures from supercritical conditions.

The cholesterol cluster is well defined and stable at $T=400$ K, while at $T=490$ the evaporation of single cholesterol molecules is observed even during relatively short simulations of 200 ps. For this reason, in what follows the discussion concerns the $T=400$ K data only. Evaporation is not observed at $T=400$ K, but the stability of Ch_{30} appears to be marginal, as shown by large fluctuations in the cluster geometry. This might be due to the high solvation potential of supercritical CO_2,[18,37] well documented in the experimental literature, especially at the fairly high temperature of the simulation. However, the marginal stability of the aggregate might also be due, at least partly, to a residual overestimation of the cholesterol/CO_2 attractive interaction.

Despite the large fluctuations, we can observe and quantify a few relevant properties for the cholesterol cluster. First of all, the discoidal character of the aggregates is lost at the conditions of these last simulations. In other words, the oblate signature in the cluster morphology is also lost, and the principal momenta of inertia display large fluctuations, without a clear relation among each other. The Ch_{30} cluster, as expected, is fluid and in fact very disordered. Again as ex-

pected, the plot of the density of atoms around the center of mass is virtually structureless and displays a broad CO_2/cholesterol interface ($\Delta_{10}^{90}=10$ Å). Comparison with the density distribution for the oxygen of CO_2 shows that cholesterol and CO_2 mix considerably at supercritical conditions, and even in the vicinity of the cluster center of mass, the CO_2 concentration is not negligible. Because of this mixing and also because of thermal expansion, the average density of cholesterol close to the center is ~10% less than the density of the crystal phase at standard conditions.

V. SUMMARY AND CONCLUSIONS

Pure cholesterol at near ambient temperature gives rise to two crystal forms both consisting of the regular stacking of bilayers in which molecules lie parallel to each other, with their tails occupying the central portion of the bilayer and the OH terminations all pointing outward. Bilayers are stitched together through their OH termination, giving rise to extended chains of hydrogen bonds, each joining molecules arranged on the opposite side of the plane separating adjacent bilayers.

Geometry optimization based on an empirical force field potential and carried out by MC annealing shows that the basic structural motifs characterizing the crystal structure appear very soon in the growth sequence of gas-phase cholesterol clusters. Low-energy structures of nanometric aggregates with $N=13$ molecules, for instance, display a clear partition of cholesterol on the two opposite sides of a common layer on which molecules converge with their OH terminations, giving rise to chains and rings of hydrogen bonds. The similarity with the crystal phases is enhanced by the nearly parallel orientation of all cholesterol molecules due to the elongated shape of cholesterol and anticipating the important role of its liquid-crystal phases. The juxtaposition of molecules of opposite orientation interacting by their OH terminations reduces lateral crowding and favors the formation of contiguous hydrogen bonds giving rise to extended structures.

The growth sequence emphasizes that the basic cohesive element in clusters and, very likely, in crystals is given by the planar arrangement of cholesterol-cholesterol hydrogen bonds. This observation, together with the analysis of the different stages of self-organization during the annealing, suggests that a basic step of nucleation and growth is represented by the condensation of an extended network of hydrogen bonds. In our simulations, this takes place at $T \sim 320$ K. It is tempting to speculate that for extended systems this event represents the driving force triggering the liquid to solid transition. It is also important to note that for $N>6$, the energy of the hydrogen bonds represents only ~25% of the cluster cohesive energy, but it is also the contribution whose structural sensitivity is the highest.

Several other less prominent features are highlighted by the results of the geometry optimization. A pair of cholesterol molecules, for instance, tends to join along their flat α-side before aggregating into larger units. Both parallel and antiparallel molecular pairs are observed and appear as relevant structural motifs in medium-size clusters. They appear also in the results of simulations for extended bilayers *in* and *on* water. Computations reveal also a fairly wide variety of defects, including misoriented molecules pointing in the direction opposite to the prevalent local orientation and molecules lying in the equatorial plane of the cluster, wrapped around the disk defined by the OH groups and by their hydrogen bonds.

The fairly weak cholesterol-cholesterol binding energy, together with the amphiphilic character of this molecule, makes cholesterol clusters very sensitive to solvation. Relatively short simulations for medium-size clusters in water and in supercritical carbon dioxide show that, as expected, drastic and opposite effects result from embedding cholesterol into a medium able to form hydrogen bonds such as water or into a hydrophobic fluid (supercritical CO_2) preferentially binding to the hydrocarbon body and tail of cholesterol. In both cases, clusters are more rounded than in the gas phase. In water at near ambient conditions, however, clusters of up to 40 molecules still display a residual discoidal character. Molecules, on average, are nearly parallel and arranged on two planes. This time, however, the hydrocarbon tails of cholesterol occupy the center of the bilayer, which exposes two circular and relatively flat hydrophilic surfaces to the water environment. The important aspect therefore is still hydrogen bonding, in this case, however, between cholesterol and water. The small size of the aggregates, nevertheless, prevents the formation of a continuous and complete hydrophilic surface able to protect the hydrocarbon bodies and tails from contact with water that instead occurs at the lateral surface of the discoidal aggregates. Larger sizes are apparently needed for the generation of well formed micelles. Clusters made of ten cholesterol molecules, however, appear to be stable in water up to $T=350$ K, thus establishing an upper bound for the saturation density at the condition of our simulations. This result is consistent with experimental data,[7] showing that the solubility of single cholesterol molecules in water is very limited. Plots of the density distribution around the center of mass of the cluster confirm that clusters are fluidlike already at $T=320$ K, as suggested also by the high relative mobility of molecules. Moreover, the cluster boundary is fairly broad ($\Delta_{10}^{90}=5\pm1$ Å), and the majority of the OH groups reside at the interface with water.

At the temperature and pressure of supercritical CO_2, instead, OH groups are spread all over the cholesterol cluster, with only a few hydrogen bonds surviving. The cluster shape fluctuates significantly and rapidly, but up to $T=400$ K the cholesterol aggregate retains its identity over the nanosecond time scale of our simulations.

The results of the present investigation suggest several directions of further exploration. First of all, anhydrous cholesterol crystals are known to spontaneously absorb water at ambient conditions, transforming into cholesterol monohydrate. It would be interesting to investigate how the addition of water affects the stability and growth pattern of nanometric cholesterol aggregates. Unfortunately, this investigation poses significant challenges since the combination of small- (water) and medium-size (cholesterol) molecules greatly decreases the efficiency of our MC sampling, undermining the applicability of our structural optimization procedure.

For cholesterol solvated in water, the primary target of further investigations will be the identification of the transition size from clusters to micelles, i.e., to aggregates exposing a continuous and complete hydrophobic surface to the water environment. This could have important implications for understanding the nucleation of cholesterol gallstones that, however, in real biological processes involves several other ingredients, such as electrolytes, proteins, and biomembranes.[38] Moreover, for clusters solvated into CO_2, the computation of thermodynamic properties as a function of size could provide data to characterize and understand extraction processes aiming at lowering the cholesterol content of food.[19]

Already at this stage, however, the results of our computations provide useful information to understand the basic steps of cholesterol aggregation that, in turn, plays an important role in important biological processes. Moreover, we hope that our results will motivate experimental investigations of these systems. Molecular beam techniques and spectroscopy measurements for single molecules in an electrostatic trap have been carried out on system of even greater complexity than cholesterol clusters. In the case of cholesterol clusters, experiments of this kind could provide quantitative information on the structure and dynamics over a wide range of size and thermodynamic conditions.

ACKNOWLEDGMENTS

We thank Dr. Mario G. Del Pópolo for several useful discussions and for carefully reading the manuscript.

[1] L. Stryer, *Biochemistry*, 4th ed. (Freeman, New York, 1995).
[2] D. M. Small and G. G. Shipley, Science **185**, 222 (1974); S. S. Katz, G. G. Shipley, and D. M. Small, J. Clin. Invest. **58**, 200 (1976).
[3] D. J. Burgess, in *Encyclopedia of Pharmaceutical Technology*, 2nd ed., edited by J. Swarbrick and J. C. Boylan (Marcel Dekker, New York, 2002); C. M. O'Driscoll and B. T. Griffin, Adv. Drug Deliv. Rev. **60**, 617 (2008).
[4] J. R. Philippot, P. G. Milhaud, C. O. Puyal, and D. F. H. Wallach, in *Liposomes as Tools in Basic Research and Industry*, edited by J. R. Philippot and F. Schuber (CRC, Boca Raton, 1995), pp. 41–75.
[5] A. V. Ambade, E. N. Savarian, and S. Thayumanavan, Mol. Pharmacol. **2**, 264 (2005); S. Basu, D. R. Vutukuri, and S. Thayumanavan, J. Am. Chem. Soc. **127**, 16794 (2005).
[6] M. A. R. B. Castanho, W. Brown, and M. J. E. Prieto, Biophys. J. **63**, 1455 (1992).
[7] M. E. Haberland and J. A. Reynolds, Proc. Natl. Acad. Sci. U.S.A. **70**, 2313 (1973).
[8] Low temperature phase: H.-S. Shieh, L. G. Hoard, and C. E. Nordman, Nature (London) **267**, 287 (1977); H.-S. Shieh, L. G. Hoard, and C. E. Nordman, Acta Crystallogr., Sect. B: Struct. Crystallogr. Cryst. Chem. **37**, 1538 (1981) High temperature phase: L.-Y. Hsu, J. W. Kampf, and C. E. Nordman, Acta Crystallogr., Sect. B: Struct. Sci. **58**, 260 (2002).
[9] H. L. Spier and K. G. van Senden, Steroids **6**, 871 (1965); K. van Putte, W. Skoda, and M. Petroni, Chem. Phys. Lipids **2**, 361 (1968) N. N. Petropavlov and N. F. Kostin, Sov. Phys. Crystallogr. **21**, 8 (1976); E. Dubler and B. Kamber, *Thermal Analysis: Proceedings of the Sixth International Conference on Thermal Analysis* (Birkhäuser, Basel, 1980).
[10] S. Kumar, S. J. Burns, and T. N. Blanton, J. Mater. Res. **10**, 216 (1995).
[11] B. M. Craven, Nature (London) **260**, 727 (1976).
[12] C. R. Loomis, G. G. Shipley, and D. M. Small, J. Lipid Res. **20**, 525 (1979); L. F. Fieser, J. Am. Chem. Soc. **75**, 5421 (1953); P. Blandon, in *Cholesterol*, edited by R. P. Cook (Academic, New York, 1958), p. 24.
[13] See, for instance, pictures reported in V. Uskoković, Steroids **73**, 356 (2008), and in Ref. 10.
[14] V. Uskoković and E. Matijević, J. Colloid Interface Sci. **315**, 500 (2007), and references therein.
[15] X. Liao and T. S. Wiedmann, Pharm. Res. **23**, 2413 (2006).
[16] M. C. Frincu, S. D. Fleming, A. L. Rohl, and J. A. Swift, J. Am. Chem. Soc. **126**, 7915 (2004).
[17] G. Troup, T. N. Tulenko, S. P. Lee, and S. P. Wrenn, Colloids Surf., B **29**, 217 (2003); J. Y. Huang, J. T. Buboltz, and G. W. Feigenson, Biochim. Biophys. Acta **1417**, 89 (1999).
[18] R. W. Randolph, D. S. Clark, H. W. Blanch, and J. M. Prausnitz, Proc. Natl. Acad. Sci. U.S.A. **85**, 2979 (1988).
[19] G. W. Froning, R. L. Wehling, S. L. Cuppett, M. M. Pierce, L. Niemann, and D. K. Siekman, J. Food Sci. **55**, 95 (1990); C.-T. Shen, S.-L. Hsu, and C.-M. J. Chang, Sep. Purif. Technol. **60**, 215 (2008); Z. Huang, S. Kawi, and Y. C. Chiew, J. Supercrit. Fluids **30**, 25 (2004).
[20] C. A. Eckert, B. L. Knutson, and P. G. Debenedetti, Nature (London) **383**, 313 (1996).
[21] D. Hermsdorf, S. Jauer, and R. Signorell, Mol. Phys. **105**, 951 (2007).
[22] S. R. T. Cromie, M. G. Del Pópolo, and P. Ballone, J. Phys. Chem. B **113**, 4674 (2009).
[23] R. Antoine, I. Compagnon, D. Rayane, M. Broyer, P. Dugourd, N. Sommerer, M. Rossignol, D. Pippen, F. C. Hagemeister, and M. F. Jarrold, Anal. Chem. **75**, 5512 (2003); Ph. Dugourd, R. Antoine, G. Breaux, M. Broyer, and M. F. Jarrold, J. Am. Chem. Soc. **127**, 4675 (2005).
[24] L. Joly, R. Antoine, A. L. Allouche, and Ph. Dugourd, J. Phys. Chem. A **112**, 898 (2008).
[25] I. Solomonov, M. J. Weygand, K. Kjaer, H. Rapaport, and L. Leiserowitz, Biophys. J. **88**, 1809 (2005); H. Rapaport, I. Kuzmenko, S. Lafont, K. Kjaer, P. B. Howes, and J. Als-Nielsen, *ibid.* **81**, 2729 (2001); S. Lafont, H. Rapaport, G. J. Sömjen, A. Renault, P. B. Howes, K. Kjaer, J. Als-Nielsen, L. Leiserowitz, and A. Lahav, J. Phys. Chem. B **102**, 761 (1998).
[26] A. Javed, M. Akram, and M. I. Shafiq, Rom. J. Physiol. **51**, 819 (2006).
[27] Z. Cournia, A. C. Vaiana, G. M. Ullmann, and J. C. Smith, Pure Appl. Chem. **76**, 189 (2004); Z. Cournia, J. C. Smith, and G. M. Ullmann, J. Comput. Chem. **26**, 1383 (2005).
[28] W. Smith, M. Leslie, and T. R. Forester, DL_POLY, Version 2.14, Daresbury Laboratories, Daresbury, Warrington, UK, 2003.
[29] D. J. Wales, *Energy Landscapes* (Cambridge University Press, Cambridge, 2003); D. J. Wales and H. A. Scheraga, Science **285**, 1368 (1999).
[30] Y. J. Wu, H. L. Tepper, and G. A. Voth, J. Chem. Phys. **124**, 024503 (2006).
[31] J. J. Potoff and J. I. Siepmann, AIChE J. **47**, 1676 (2001).
[32] P. G. de Gennes and P. J. Prost, *The Physics of Liquid Crystals*, 2nd ed. (Oxford University Press, New York, 1993).
[33] S. R. T. Cromie, M. G. Del Pópolo, and P. Ballone, "Dense cholesterol layers on the water surface" (unpublished).
[34] Z. Wang and X. He, J. Chem. Phys. **130**, 094905 (2009).
[35] M. Cano-Sarabia, N. Ventosa, S. Sala, C. Patio, R. Arranz, and J. Veciana, Langmuir **24**, 2433 (2008).
[36] R. Span and W. Wagner, J. Phys. Chem. Ref. Data **25**, 1509 (1996).
[37] A. Akgerman and G. Madras, in *Supercritical Fluids: Fundamentals and Applications*, edited by E. Kiran and J. M. H. L. Sengers (Kluwer, Dordrecht, 1994); G. Madras, Fluid Phase Equilib. **220**, 167 (2004).
[38] A. Coello, F. Meijide, E. Rodríguez Núñez, and J. V. Tato, J. Pharm. Sci. **85**, 9 (1996).